

See discussions, stats, and author profiles for this publication at: <https://www.researchgate.net/publication/249998379>

jp308455y

DATASET · JULY 2013

READS

23

3 AUTHORS, INCLUDING:



Ki Wi Chen

Tunghai University

12 PUBLICATIONS 117 CITATIONS

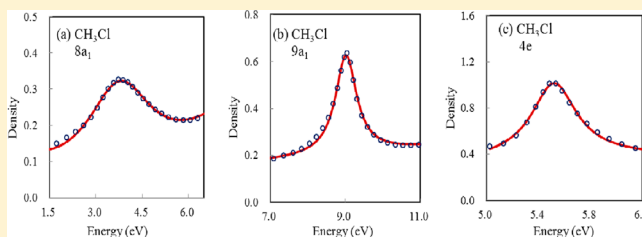
SEE PROFILE

Energies and Lifetimes of Temporary Anion States of Chloromethanes by Stabilized Koopmans' Theorem in Long-Range Corrected Density Functional Theory

Hsiu-Yao Cheng* and Chi-Wei Chen

Department of Chemistry, Tunghai University, Taichung 40704, Taiwan, R.O.C.

ABSTRACT: To investigate the resonance energies and lifetimes of temporary anion states of chloromethanes, long-range corrected density functional theory is adopted in this article. Their values are determined by calculating the density of resonance states via the stabilized Koopmans' theorem. The characteristics of these resonance orbitals are also analyzed. By comparing with experimental values and previous theoretical calculations, our method can yield not only conformable results but also more complete information on the resonance states.



1. INTRODUCTION

Chloromethanes, as the prototypical molecules of chlorinated hydrocarbons, have been widely used in organic synthesis, pharmaceuticals, material science, and surface and industrial chemistry.¹ Temporary or metastable anion states² play an important role in studying the bonding, chemical properties, and dissociative attachment of chlorinated hydrocarbons. They can be observed as a sharp resonance in the electron-molecule scattering cross-section by electron transmission spectroscopy (ETS)³ technique. Burrow et al. have carried out ETS measurements for chloromethanes, and they have found the low-lying C–Cl σ^* resonances for these compounds.⁴ Previous works of dissociative electron attachment, scattering cross-section, inner-shell electron excitation, and theoretical studies have also reported the electron attachment energies for the formation of temporary anions of chloromethanes.^{5–9} However, there exists controversy about the assignments of C–Cl σ^* resonances of chloromethanes. Falcetta and Jordan have identified the C–Cl σ^* resonances via stabilization calculation and confirmed the assignments of the features observed in ET spectrum made by Burrow et al.⁸ On the basis of MS- $X\alpha$ calculation, Guerra et al. have further supported their assignments.⁹

The vertical attachment energies (AEs) are commonly computed via Koopmans' theorem (KT)¹⁰ approximation. They are associated with the unfilled molecular orbital energies. Nevertheless, the energy calculations of temporary anion states using the KT approximation are unreliable. When small basis sets are used, the relative energies of temporary anion states cannot be accounted for by the KT approximation. The reason is mainly due to the artificial binding of the electron by the compact basis set. In addition, neither of the large basis sets KT calculations can provide definitive energies of temporary anion states. This is because temporary anions lie in the continuum of neutral molecule plus a free electron. The temporary anion

resonance states are likely to collapse onto approximations of continuum functions called orthogonalized discretized continuum (ODC)^{11–13} solutions. To distinguish the resonance solutions from the ODC ones, the stabilization method proposed by Taylor and co-workers¹⁴ can be employed. Jordan and co-workers have applied the stabilization method in conjunction with KT within the HF theory to assign the temporary anion states for several molecules.^{12,15} Their stabilized Koopmans' theorem (SKT) approach is generally very successful in predicting the relative AEs of isolated molecules when using flexible basis sets.^{15,16} When using the density functional theory (DFT)¹⁷ method, most DFT potentials will not yield asymptotic behavior properly.^{2a,18} The errors for Koopmans' AEs in conventional DFT can be of several electron volts. To reduce the errors, Tozer and De Proft have suggested an asymptotic correction (AC) to the Koopmans expression based on the consideration of the integer discontinuity in the exact exchange-correlation potential.¹⁹ Alternatively, the long-range corrected (LRC) DFT can also be adopted for AC.^{20–23} We have recently applied the stabilization method within DFT employing asymptotically corrected potential to study the temporary anion states of several different molecules.²⁴ Results have indicated that our approach can improve the accuracy in predicting energies of temporary anion states.

So far, the $\sigma^*_{\text{C–Cl}}$ resonances of chloromethanes have been identified.^{4,8,9} Yet, the identification of $\sigma^*_{\text{C–H}}$ resonances is lacking. In addition, theoretical studies for the resonance lifetimes of chlorinated hydrocarbons have been scarce. In this article, we will investigate chloromethanes via the SKT using LRC-DFT. Then, their resonance energies and lifetimes will be

Received: August 26, 2012

Revised: November 23, 2012

Published: November 28, 2012



determined by calculating the density of resonance states. Finally, the results will be compared with experimental values and previous theoretical calculations.

2. COMPUTATIONAL METHODS

The unfilled orbital energy associated with temporary anion state is known as AE. The AEs in the KT approximation can be written as $AE \approx \varepsilon_{\text{VMO}}$, where ε_{VMO} denotes the virtual molecular orbital energy. To distinguish the temporary anion state solutions from the virtual ODC ones, the SKT is employed. Four different Gaussian-type basis sets, designated as A1, A2, A3, and B are employed in our calculations. Our convention is as follows. The basis set A1 denotes the 6-311++G(d,p) basis set with scaling of the exponents of diffuse + functions on all atoms. The basis set A2 is the 6-311++G(3d,p) with scaling of the exponents of diffuse + functions on all atoms. The basis set A3 is the 6-311++G(3df,3dp) with scaling of the exponents of diffuse + functions on all atoms. Finally, the basis set B denotes the aug-cc-pvtz basis set²⁵ with scaling of the outermost diffuse s and p functions on the C, N, and O atoms and the outermost s function on the H atom.

The stabilization graphs are obtained by plotting the calculated energies ε_{VMO} as a function of the scale factor α . With sufficiently flexible basis sets, some ODC solutions may approach the temporary anion orbital solutions in energy and can lead to avoided crossings between the two types of solutions as α increases. The unfilled orbitals corresponding to the temporary anion states are referred to as SKT levels.¹¹ The energies of SKT levels can be extracted from the avoided crossings between the eigenvalues of the stabilization graph. In the study of resonance energies for all SKT calculations, the simplest midpoint method in Burrow et al. will be used first.¹² The energy of SKT level is taken as the mean value of two eigenvalues involved in the avoided crossing, if it exists, at the α_{ac} of closest approach.²⁶ The density of states (DOS) method introduced by Mandelshtam et al. will then be adopted to estimate resonance energies and widths according to the stabilization graphs.²⁷ In the present study, the DOS procedure is accomplished by using the modified version by Ho and coworkers.²⁸ The modified procedure was proven to be compatible when compared its results with the other most accurate calculations.^{28a} Instead of using the average DOS by Mandelshtam et al., the density of resonance state ρ_n for each eigenstate of stabilization graph is calculated by using the following formula

$$\rho_n(E) = \left[\frac{E_n(\alpha_{i+1}) - E_n(\alpha_{i-1})}{\alpha_{i+1} - \alpha_{i-1}} \right]_{E_n(\alpha_i)=E}^{-1} \quad (1)$$

where the index i is the i th varied α value, and n the n th eigenstate. The resonance energy E_r and resonance width Γ can then be determined by the following Lorentzian fitting

$$\rho_n(E) = \rho_a + \frac{\rho_b(\Gamma/2)}{(E - E_r)^2 + (\Gamma/2)^2} \quad (2)$$

where ρ_a is a smooth energy-dependent background and ρ_b a constant to be fitted. The width is related to the lifetime τ via $\tau = \hbar/\Gamma$. Among different fitting curves for each eigenroot, the one that gives the best fit, i.e., with the least chi square, is chosen as the particular resonance.²⁸

In the present study, we adopt ω B97XD, LC- ω PBE, and CAM-B3LYP LRC functionals via SKT for the temporary anion

states. The ω B97XD²⁰ functional includes long-range (LR) HF exchange, a small fraction of short-range (SR) HF exchange, a modified B97 SR exchange, B97 correlation density functional, and empirical dispersion corrections. The LC- ω PBE²¹ functional contains SR ω PBE exchange, LR HF exchange, and full-range PBE correlation. The CAM-B3LYP²² functional comprises 0.19 HF plus 0.81 Becke 1988 (B88) exchange interaction at SR and 0.65 HF plus 0.35 B88 at LR. As for comparison, the double-hybrid functionals B2PLYP-D that contain second-order perturbation corrections with LR dispersion terms²⁹ will also be employed. All calculations are performed using the Gaussian09 program³⁰ with geometric optimization of all molecules being carried out at the B3LYP/6-311+G(d,p) level. The geometries of CH_3Cl , CH_2Cl_2 , CHCl_3 , and CCl_4 are optimized under D_{3h} , C_{2v} , C_{3v} , and T_d symmetry constraints. The symmetry in the labeling of the orbital is based on the z-axis being along the principal axis. The optimized bond lengths for the C–Cl bonds are 1.79–1.80 Å for all chloromethanes.

3. RESULTS AND DISCUSSION

First, we will present the results of CH_3Cl . In the C_{3v} point group, the CH_3Cl molecule has seven a_1 , and three-pair e occupied orbitals. For the temporary anion resonances, we perform SKT calculations for the ω B97XD, LC- ω PBE, CAM-B3LYP, and B2PLYP-D (denoted as $\text{SKT}^{\omega\text{B97XD}}$, $\text{SKT}^{\text{LC-}\omega\text{PBE}}$, $\text{SKT}^{\text{CAM-B3LYP}}$, and $\text{SKT}^{\text{B2PLYP-D}}$, respectively) on the unfilled orbitals. In order to distinguish the resonance and ODC solutions of the molecular system, it is useful to study the so-called one-electron discretized continuum (1e-DC)^{11b,c} solutions for a free electron. The energies of the 1e-DC solutions are obtained by solving the one-electron Schrödinger equation as described by the molecular basis set in the absence of any potential.^{11b,c}

The stabilization graphs for the a_1 and e virtual orbitals of CH_3Cl and the 1e-DC solutions calculated via $\text{SKT}^{\omega\text{B97XD}}$ method using basis set A1 are shown in Figure 1. There are two types of energies for virtual orbital solutions in the stabilization calculations. One is the unfilled orbital solution and the other the ODC virtual orbital solution. By comparing the energies and characteristics of the virtual orbitals from DFT calculations of molecules with those of the 1e-DC solutions, one can determine the possible temporary anion states.^{11c} As shown in Figure 1, all 1e-DC solutions increase with α . First, we will present the results for the a_1 virtual orbitals. By examining the nature of virtual orbitals of CH_3Cl as shown in Figure 1a, the fifth solution for $0.5 < \alpha < 0.8$ and the sixth solution for $\alpha < 0.5$ are mainly from the $8a_1$ orbital solution. The fifth solution for $\alpha > 1.7$, sixth for $1.4 < \alpha < 1.7$, and seventh for $0.6 < \alpha < 1.4$ are mainly from the $9a_1$ orbital solution. For $\alpha < 1.0$, the first four solutions correspond to the first four ODC solutions. Five avoided crossings are found in Figure 1a. The two avoided crossings below 4 eV are from the couplings between $8a_1$ orbitals and the fourth and fifth ODC solutions. The locations of them are at $\alpha_{\text{ac}}(4,5) = 0.8$ and $\alpha_{\text{ac}}(5,6) = 0.5$, respectively. Their corresponding energies are 3.60 eV at $\alpha_{\text{ac}}(4,5)$ and 3.40 eV at $\alpha_{\text{ac}}(5,6)$. The average value from each set will be defined as the energy of the temporary anion state. Thus, after taking the average, the energy of the $8a_1$ orbitals is 3.50 eV. As for the other three avoided crossings, they are from the couplings between $9a_1$ orbital and the ODC solutions. The energies of $9a_1$ orbital obtained are 8.15, 8.60, and 9.35 at $\alpha_{\text{ac}}(5,6) = 1.7$, $\alpha_{\text{ac}}(6,7) = 1.4$, and $\alpha_{\text{ac}}(7,8) = 0.6$,

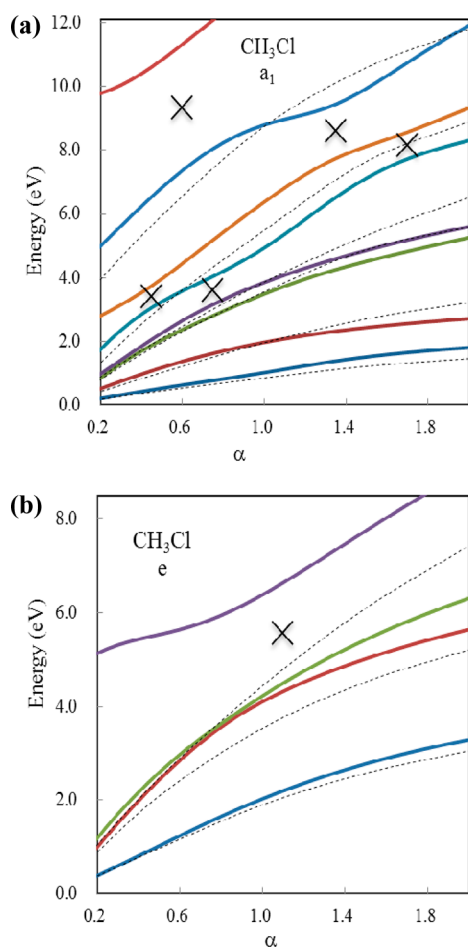


Figure 1. Stabilization graphs for CH_3Cl via $\text{SKT}^{\omega\text{B97XD}}$ method using basis set A1. Energies of (a) a_1 and (b) e virtual orbitals (represented by the solid curves) and the free electron (represented by the dashed curves) as a function of α . The locations of α_{ac} are marked with \times .

respectively. Hence, the energy of the $9a_1$ orbital is 8.70 eV. In Figure 1b, the stabilization graph has one e resonance solution. The fourth solution for $\alpha < 1.1$ is mainly from the $4e$ orbital solution. The energies of the $4e$ obtained from the avoided crossing is 5.57 eV at $\alpha_{ac}(3,4) = 1.1$. On the basis of our analysis of the $8a_1$, $9a_1$, and $4e$ SKT orbitals, the LUMO $8a_1$ is essentially from C–Cl σ^* . The $9a_1$ orbital is mainly from σ^*_{CH} . The $4e$ orbitals are essentially from CH_3 pseudo- π^* , which resulted from the antibonding of C ($2p_{xy}$) with H ($1s$).

As for CH_2Cl_2 molecule, it has nine a_1 , two a_2 , three b_1 , and seven b_2 occupied orbitals in the C_{2v} point group. The stabilization graphs of CH_2Cl_2 for the a_1 , b_1 , and b_2 virtual orbitals and the 1e-DC solutions via $\text{SKT}^{\omega\text{B97XD}}$ method using basis set A1 are shown in Figure 2. For the a_1 virtual orbitals as shown in Figure 2a, the first solution is mainly from the first a_1 ODC solution. The sixth solution for $0.2 < \alpha < 0.3$ and seventh for $\alpha < 0.2$ are mainly from the $10a_1$ orbital solution. The sixth solution for $\alpha > 1.8$, seventh for $1.3 < \alpha < 1.8$, and eighth for $0.8 < \alpha < 1.3$ are mainly from the $11a_1$ orbital solution. The energy of the $10a_1$ orbital obtained is 1.50 eV at $\alpha_{ac}(6,7) = 0.2$. The energies obtained for $11a_1$ orbital are 7.69 eV at $\alpha_{ac}(6,7) = 1.8$, 7.80 eV at $\alpha_{ac}(7,8) = 1.3$, and 9.57 eV at $\alpha_{ac}(8,9) = 0.8$. Thus, the energy of the $11a_1$ orbital is 8.35 eV. In Figure 2b, the first and second solutions are mainly from the first and second b_1 ODC solutions. The third solution for $\alpha > 1.2$ and the fourth

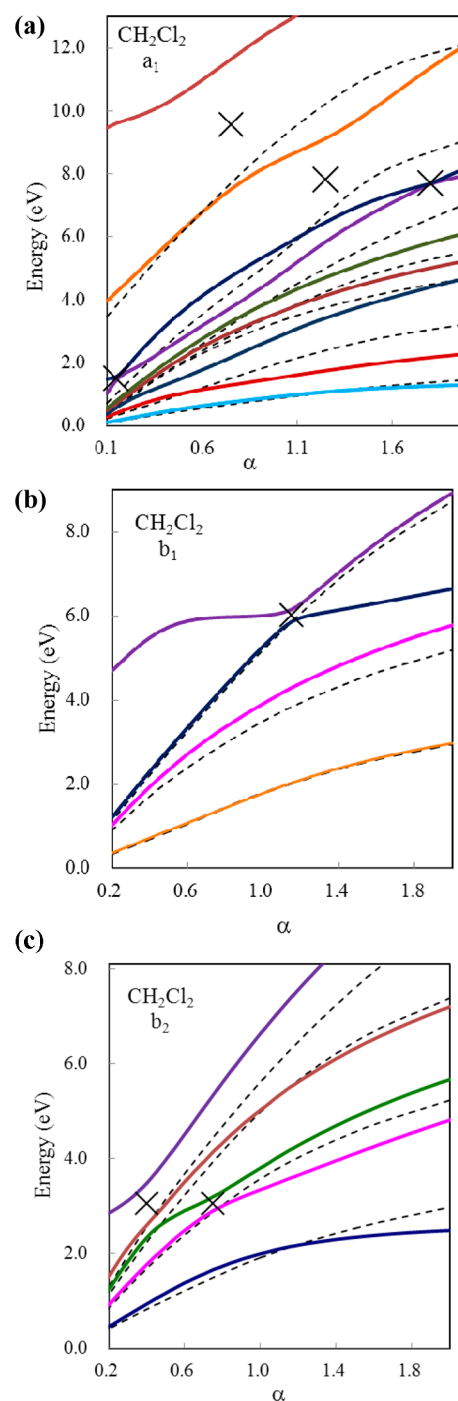


Figure 2. Stabilization graphs for CH_2Cl_2 via $\text{SKT}^{\omega\text{B97XD}}$ method using basis set A1. Energies of (a) a_1 , (b) b_1 , and (c) b_2 virtual orbitals (represented by the solid curves) and the free electron (represented by the dashed curves) as a function of α . The locations of α_{ac} are marked with \times .

solution for $0.5 < \alpha < 1.2$ are mainly from the $4b_1$ orbital solution. The energy of the $4b_1$ orbital obtained is 6.01 eV at $\alpha_{ac}(3,4) = 1.2$. Similarly, for the b_2 virtual orbitals as shown in Figure 2c, the energies of the $8b_2$ orbital obtained are 3.05 and 3.04 eV at $\alpha_{ac}(2,3)$ and $\alpha_{ac}(4,5)$, respectively. Hence, the energy of the $8b_2$ orbital is 3.05 eV. On the basis of our analysis of the $10a_1$, $11a_1$, $4b_1$, and $8b_2$ SKT orbitals, the $10a_1$ and $8b_2$ orbitals are mainly from C–Cl σ^* . The $4b_1$ orbital is mainly from CH_2 pseudo π^* . The $11a_1$ orbital is mainly from C–H σ^* .

Next, for the CHCl_3 molecule, it has nine a_1 , two a_2 , and nine-pair e occupied orbitals in the C_{3v} point group. The stabilization graphs of CHCl_3 for the a_1 and e virtual orbitals and the 1e-DC solutions via $\text{SKT}^{\omega\text{B97XD}}$ method using basis set A1 are shown in Figure 3. In Figure 3a, the first solution for $\alpha >$

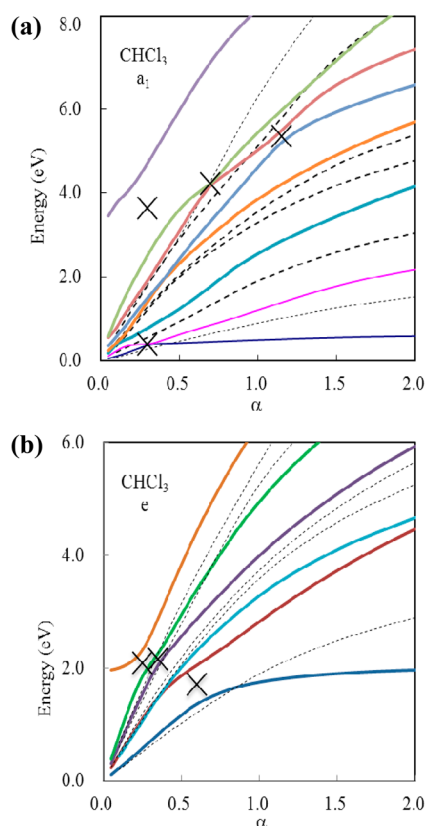


Figure 3. Stabilization graphs for CHCl_3 via $\text{SKT}^{\omega\text{B97XD}}$ method using basis set A1. Energies of (a) a_1 and (b) e virtual orbitals (represented by the solid curves) and the free electron (represented by the dashed curves) as a function of α . The locations of α_{ac} are marked with \times .

0.4 and the sixth solution for $0.7 < \alpha < 1.0$ are mainly from the $10a_1$ and $11a_1$ orbital solutions, respectively. The energies obtained for $10a_1$ orbital is 0.38 eV at $\alpha_{ac}(1,2) = 0.3$. The energies obtained for $11a_1$ orbital are 5.34 eV at $\alpha_{ac}(5,6) = 1.2$, 4.20 eV at $\alpha_{ac}(6,7) = 0.7$, and 3.62 eV at $\alpha_{ac}(6,7) = 0.3$. Thus, the energy of the $11a_1$ orbital is 4.39 eV. In Figure 3b, the first solution for $\alpha > 0.6$ is mainly from the $10e$ orbital solution. The energies obtained for $10e$ orbitals are 1.71 eV at $\alpha_{ac}(1,2) = 0.6$, 2.16 eV at $\alpha_{ac}(4,5) = 0.4$, and 2.09 eV at $\alpha_{ac}(6,7) = 0.3$. Hence, the energy of the $10e$ orbitals is 1.98 eV. According to our analysis of the SKT orbitals for the bonding characteristics of unfilled orbitals of CHCl_3 , the $10a_1$ and $10e$ orbitals are essentially from C–Cl σ^* . The $11a_1$ orbital is mainly from σ^*_{CH} .

For the CCl_4 molecule, it has six a_1 , two-pair e , two triply degenerate t_1 , and seven triply degenerate t_2 occupied orbitals in the T_d point group. The stabilization graphs of CCl_4 for the a_1 and t_2 virtual orbitals and the 1e-DC solutions via $\text{SKT}^{\omega\text{B97XD}}$ method using basis set A1 are shown in Figure 4. As shown in Figure 4a, the energy of the $7a_1$ lies below zero (~ -0.18 eV). In Figure 4b, the first solution for $\alpha > 0.4$ is mainly from the $8t_2$ orbital solution. The energies obtained for $8t_2$ orbitals are 1.09 eV at $\alpha_{ac}(1,2) = 0.4$ and 1.23 eV at $\alpha_{ac}(2,3) = 0.3$. Hence, the

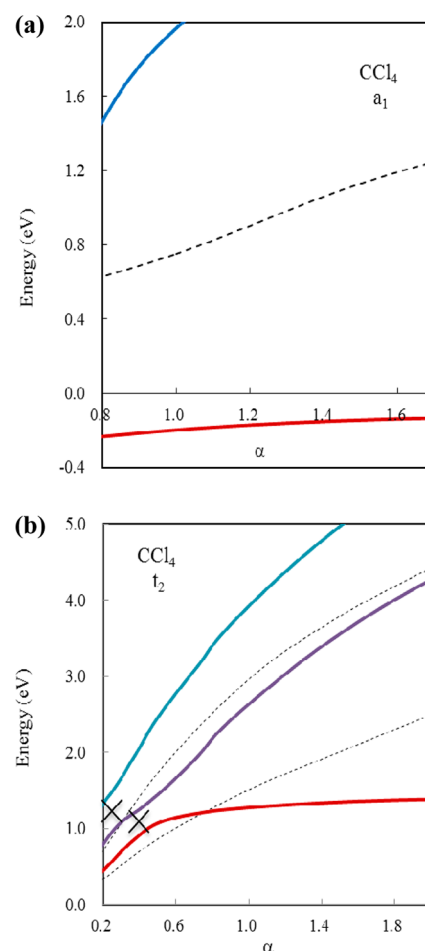


Figure 4. Stabilization graphs for CCl_4 via $\text{SKT}^{\omega\text{B97XD}}$ method using basis set A1. Energies of (a) a_1 and (b) t_2 virtual orbitals (represented by the solid curves) and the free electron (represented by the dashed curves) as a function of α . The locations of α_{ac} are marked with \times .

energy of the $8t_2$ orbitals is 1.16 eV. According to our analysis, the $7a_1$ and $8t_2$ orbitals are all from $\sigma^*_{\text{C-Cl}}$.

The calculated AEs of chloromethanes using basis set A1 are tabulated along with the experimental values in Table 1. To compare with experimental results, corrected AEs are also included in the table. The corrected values are obtained by shifting the amount from the calculated AE values to bring the LUMO of CH_3Cl into agreement with the experimental values of Burrow et al.⁴ From the table, it can be seen that the AEs obtained via the $\text{SKT}^{\text{LC-}\omega\text{PBE}}$ and $\text{SKT}^{\omega\text{B97XD}}$ methods are larger than those obtained from the $\text{SKT}^{\text{CAM-B3LYP}}$ and $\text{SKT}^{\text{B2PLYP-D}}$ methods. Notice that the AEs obtained from previous SKT HF/6-31+G method have already been shifted by -3.15 eV in their paper. Hence, the AEs obtained from previous SKT^{HF} method are larger than those obtained from all of the DFT methods. These discrepancies are possibly due to the different considerations of asymptotic exchange-correlation potential, self-interaction effect, long-range dispersion corrections, and asymptotic Coulomb contributions.³¹ Table 2 lists the results of calculated AEs of CH_3Cl using different basis sets for the representative $\text{SKT}^{\omega\text{B97XD}}$ method. Notice that all basis sets have polarization functions. The AEs vary within 0.2 eV for unfilled orbitals in all basis sets. Our calculations have revealed that the 6-311++G(d,p) basis set A1 is sufficiently flexible to characterize the anion states of CH_3Cl . The inclusion of

Table 1. Calculated and Corrected^a AEs (eV) for Chloromethanes Using Basis Set A1

method	CH ₃ Cl			CH ₂ Cl ₂				CHCl ₃			CCl ₄	
	8a ₁	4e	9a ₁	10a ₁	8b ₂	4b ₁	11a ₁	10a ₁	10e	11a ₁	7a ₁	8t ₂
SKT ^ω B97XD	3.50 (3.45)	5.57 (5.52)	8.70 (8.65)	1.50 (1.45)	3.05 (3.00)	6.01 (5.96)	8.35 (8.30)	0.38 (0.33)	1.98 (1.93)	4.39 (4.34)	−0.20 (−0.25)	1.16 (1.11)
SKT ^{LC-ω} PBE	3.62 (3.45)	5.76 (5.59)	8.89 (8.72)	1.67 (1.50)	3.25 (3.08)	6.21 (6.04)	8.51 (8.34)	0.61 (0.44)	2.12 (1.95)	4.57 (4.40)	0.03 (−0.14)	1.52 (1.35)
SKT ^{CAM-B3} LYP	2.74 (3.45)	4.77 (5.48)	7.97 (8.68)	0.73 (1.44)	2.29 (3.00)	5.27 (5.98)	7.60 (8.31)	−0.31 (0.40)	1.20 (1.91)	3.61 (4.32)	−1.25 (−0.54)	0.43 (1.14)
SKT ^{B2PLYP} -D	2.90 (3.45)	4.95 (5.50)	8.10 (8.65)	0.90 (1.45)	2.43 (2.98)	5.45 (6.00)	7.74 (8.29)	−0.07 (0.48)	1.41 (1.96)	3.73 (4.28)	−0.97 (−0.42)	0.75 (1.30)
SKT (HF/6-31+G) ^b	3.55			1.15	3.35			0.35	1.95		−1.10	1.05
MS-Xα ^c	3.25			1.51	2.68			0.36	1.84		−0.50	0.94
exptl ^d	3.45			1.23	3.38			0.35	1.83		<0	0.94
exptl ^e	3.5	5.5	8.5									

^aThe corrected values (shown in parentheses) are obtained by shifting the amount needed to bring the calculated AEs into agreement with the experimental values of ref 4 for the LUMO of CH₃Cl. ^bRef 8. ^cRef 9. ^dRef 4. ^eRef 5d.

Table 2. Calculated AEs (eV) for CH₃Cl Using SKT^ωB97XD Method

basis set	8a ₁	4e	9a ₁
A1	3.50	5.57	8.70
A2	3.51	5.53	8.71
A3	3.40	5.47	8.67
B	3.46	5.44	8.80

additional diffuse d or f polarization functions on C is of minor importance. Previous SKT HF studies by Falcetta and Jordan have also indicated that the 6-31+G(d) basis set is sufficiently flexible to describe the unfilled orbitals of chloromethanes.⁸

Now for resonance energy and width, the density of resonance states ρ_n for each virtual orbital near the stabilization plateau is calculated using eq 1. The calculated values of ρ_n are then fitted to eq 2, and the one that gives the best fit to the Lorentzian form is chosen as our result.²⁸ For instance, for the 9a₁ resonance of CH₃Cl in Figure 1a, only the 5th to 7th solutions are associated with it. Therefore, only the 5th–7th solutions are used for DOS calculation and fitting for 9a₁. According to the fitting results, the 7th solution is chosen as the result of 9a₁ orbital since it gives better Lorentzian fitting than those obtained from the 5th and 6th solutions. The resonance parameters for the other unfilled orbitals of chloromethanes have been analyzed in a similar fashion as 9a₁ of CH₃Cl. Figure 5 shows the DOS for the 8a₁, 9a₁, and 4e orbitals of CH₃Cl. The 4e orbitals are from the 4th e orbital solution of stabilization graph (Figure 1b). From the fit, the resonance energies and widths obtained are 3.76 and 2.64 eV for 8a₁ orbital, 9.02 and 0.68 eV for 9a₁ orbital, and 5.52 and 0.42 eV for 4e orbital, respectively. Figure 6 shows the DOS for the 10a₁, 11a₁, 4b₁, and 8b₂ orbitals of CH₂Cl₂. They are from the 3rd and 8th a₁ solutions in Figure 2a, the 4th b₁ solution in Figure 2b, and 3rd b₂ solution in Figure 2c. The resonance energies and widths obtained are 1.20 and 0.96 eV for 10a₁, 8.72 and 1.41 eV for 11a₁, 5.97 and 0.04 eV for 4b₁, and 2.98 and 0.67 eV for 8b₂ orbitals, respectively. For CHCl₃, Figure 7 shows the DOS 10a₁, 11a₁, and 10e orbitals. They are from the 2nd and 7th a₁ solutions in Figure 3a, and 4th e solution in Figure 3b. The resonance energies and widths obtained are 0.39 and 0.01 eV for 10a₁, 4.02 and 0.45 eV for 11a₁, and 2.08 and 0.76 eV for 10e orbitals, respectively. For CCl₄, Figure 8 shows the DOS for the 8t₂ orbitals. They are from 2nd t₂ virtual

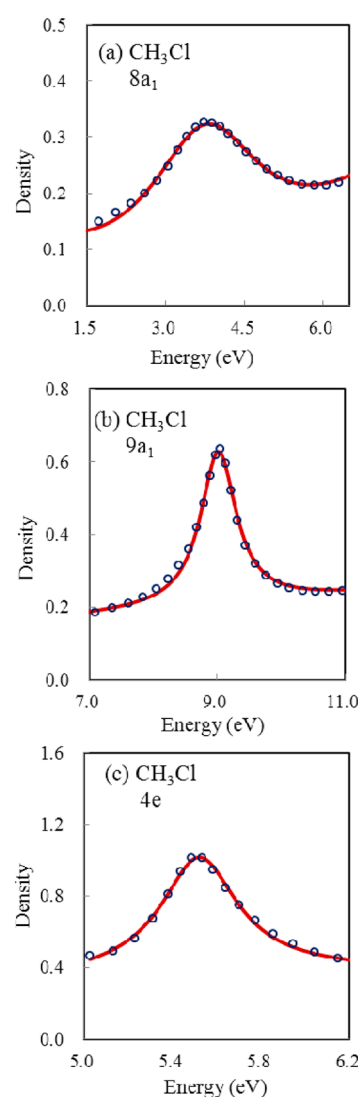


Figure 5. Calculated density (open circle) and fitted Lorentzian (solid line) for (a) 8a₁, (b) 9a₁, and (c) 4e orbitals of CH₃Cl.

orbitals of Figure 4b. The resonance energy and width obtained are 1.24 and 0.34 eV for 8t₂ orbitals, respectively.

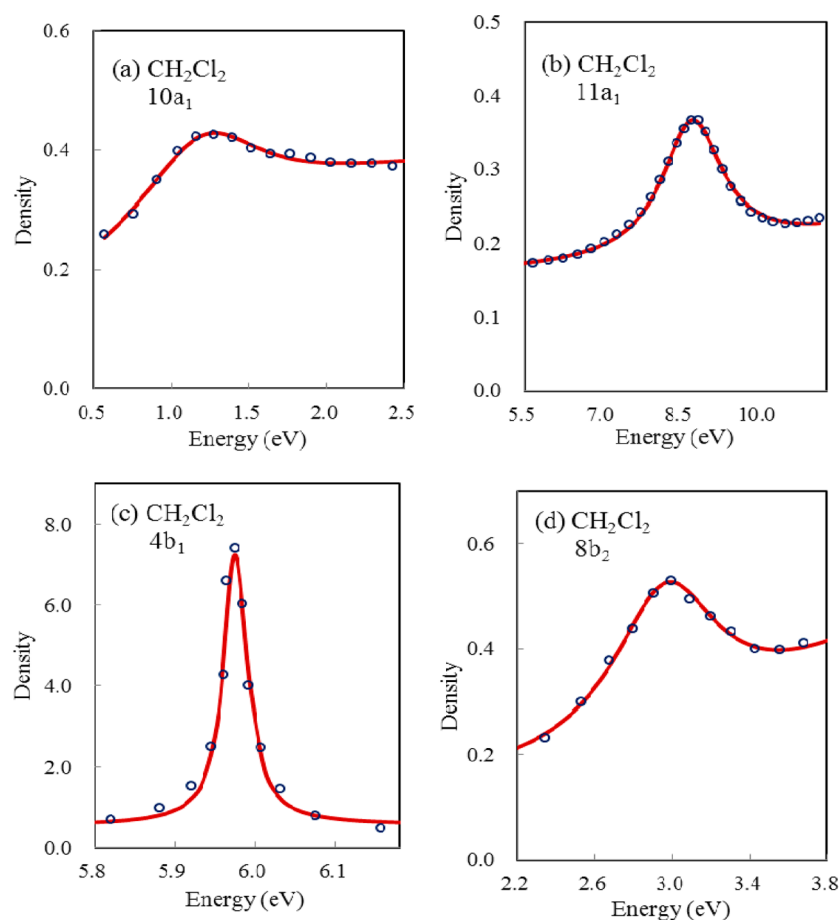


Figure 6. Calculated density (open circle) and fitted Lorentzian (solid line) for the (a) $10a_1$, (b) $11a_1$, (c) $4b_1$, and (d) $8b_2$ orbitals of CH_2Cl_2 .

The calculated DOS could be very different by using different ODC states. To compare with the aforementioned results derived from the best Lorentzian fitting curve, results derived from the average of all Lorentzian fitting curves are also studied. For CH_3Cl molecule, the obtained resonance energies and widths of the $9a_1$ orbital from the DOS analysis are 8.52 and 1.76 eV for the 5th solution, 7.87 and 1.23 eV for the 6th solution, and 9.02 and 0.68 eV for 7th solution. Thus, the average energy and width of the $9a_1$ orbital are 8.47 and 1.22 eV. As for the $8a_1$ and $4e$ orbitals since there is only one ODC solution associated with each one of them, so their average values are the same. For CH_2Cl_2 molecule, the obtained resonance energies and widths of the $10a_1$ orbital are 1.24 and 0.71 eV for the 2nd solution, 1.20 and 0.96 eV for the 3rd solution, and 1.82 and 0.67 eV for the 6th solution. Thus, the average energy and width of the $10a_1$ orbital are 1.42 and 0.78 eV. The resonance energies and widths obtained for $11a_1$ orbital are 7.13 and 0.95 eV for the 7th solution and 8.72 and 1.41 eV for the 8th solution. Hence, the average energy and width of the $11a_1$ orbital are 7.93 and 1.18 eV. The energies and widths obtained for $4b_1$ orbital are 6.19 and 0.46 eV for the 3rd solution and 5.98 and 0.04 eV for the 4th solution. The energies and widths obtained for $8b_2$ orbital are 3.31 and 0.91 eV for the 2nd solution and 2.98 and 0.67 eV for the 3rd solution. Hence, the average energies and widths are 6.09 and 0.25 eV for $4b_1$ orbital and 3.14 and 0.79 eV for $8b_2$ orbital, respectively. As to the CHCl_3 molecule, the resonance energies and widths obtained for $10a_1$ orbital are 0.44 and 0.06 eV for the 1st solution, 0.39 and 0.01 eV for the 2nd solution, and 0.94

and 0.72 eV for 3rd solution. The average resonance energy and width are 0.59 and 0.26 eV. For $11a_1$ orbital, the resonance energies and widths obtained are 4.66 and 1.32 eV for the 6th solution and 4.02 and 0.45 eV for 7th solution. The average values are 4.34 and 0.89 eV. For $10e$ orbital, the resonance energies and widths obtained are 2.14 and 0.68 eV for the 2nd solution, 2.08 and 0.76 eV for the 4th solution, and 2.06 and 0.83 eV for the 5th solution. The average resonance energy and width are 2.09 and 0.76 eV. For the CCl_4 molecule, its resonance energies and widths obtained for $8t_2$ orbital are 1.24 and 0.35 eV for the 2nd solution and 1.48 and 0.47 eV for 3rd solution. Hence, its average resonance energy and width are 1.36 and 0.41 eV.

Table 3 tabulates all of these calculated resonance energies and widths of chloromethanes using basis set A1 for the representative SKT^{aB97XD} method along with those of previous studies.^{4,5d,e,8,9} As can be seen from the results for the resonance energies, our calculated resonance energies for the seven C–Cl σ^* resonances 2A_1 of CH_3Cl , 2A_1 and 2B_2 of CH_2Cl_2 , 2A_1 and 2E of CHCl_3 , and 2A_1 and 2T_2 of CCl_4 are in agreement with those of the previous studies by Burrow et al.,⁴ Falcetta and Jordan,⁸ and Guerra et al.⁹ As for $4e$ pseudo- $\pi^*_{\text{CH}_3}$ and $9a_1$ σ^*_{CH} orbitals of CH_3Cl , previous studies by Burrow et al. identified the resonances at 5.5 and 8.5 eV,^{5d} which were close to our calculated values. As to the resonance widths, previous studies were rather incomplete. Our calculated resonance widths for the $\sigma^*_{\text{C-Cl}}$ resonances obtained from the results derived from the average of all Lorentzian fitting curves are 2.64 eV for 2A_1 of CH_3Cl , 0.78 and 0.79 eV for 2A_1

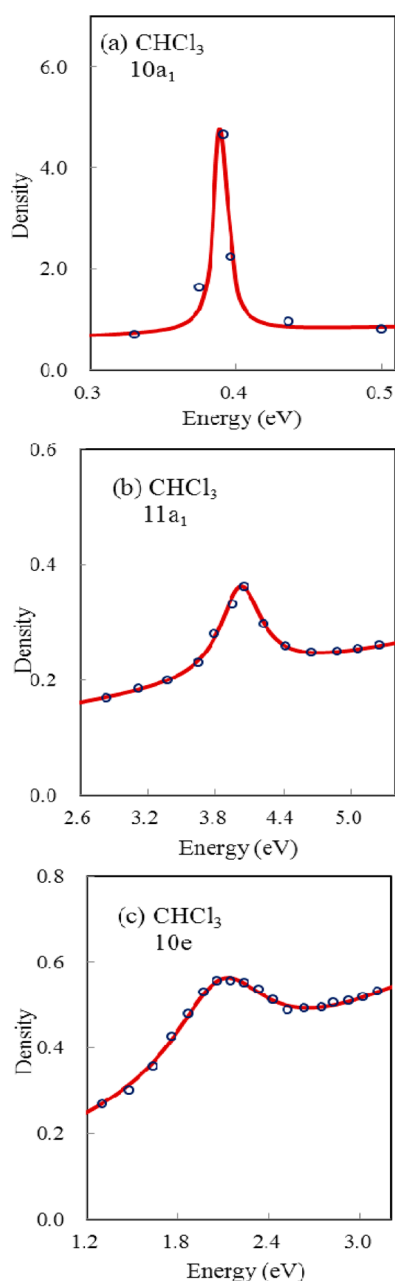


Figure 7. Calculated density (open circle) and fitted Lorentzian (solid line) for the (a) $10a_1$, (b) $11a_1$, and (c) $4e$ orbitals of CHCl_3 .

and 2B_2 of CH_2Cl_2 , 0.26 and 0.76 eV for 2A_1 and 2E of CHCl_3 , and 0.41 eV for 2T_2 of CCl_4 , respectively. Accordingly, the lifetimes for the lowest $\sigma_{\text{C-Cl}}^*$ are in the following order: CH_3Cl (~ 0.2 fs) < CH_2Cl_2 (~ 0.8 fs) < CHCl_3 (~ 2.5 fs). The lowest $\sigma_{\text{C-Cl}}^*$ energy for CCl_4 is below zero. It is noteworthy that when the results derived from the best Lorentzian fitting curve is used, the widths obtained for the $4b_1$ orbital of CH_2Cl_2 and $10a_1$ orbital of CHCl_3 are very small. Hence, the values calculated may have relatively large errors. One of the possible reasons for the errors in symmetry a_1 is that the ODC solutions have very different compositions. As shown in Table 3, the values obtained from the results derived from the average of all Lorentzian fitting curves are in agreement with those of previous studies by Burrow et al.^{4,5d,e} Notice, in particular, that the resonance energy and width for $8a_1$ orbital of CH_3Cl have also been reported by previous MP3 study of temporary

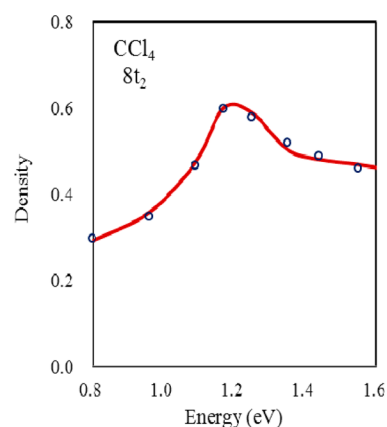


Figure 8. Calculated density (open circle) and fitted Lorentzian (solid line) for the $8t_2$ orbitals of CCl_4 .

CH_3Cl^- anion.³² The values were 2.46 and 3.98 eV when using the stabilization method in the static exchange approximation, respectively. The resonance energy was 2.40 eV when using the stabilization method in MP3 and UOVGF. In addition, the resonance energy was 2.43 eV when using the MCSCF calculations.³³ Hence, our calculated results are closer to experimental values when compared with theirs.

According to our SKT calculations for the assignments of the shape resonance observed in ET spectrum on CH_3Cl , the 3.45 eV feature is ascribed to electron capture into the empty $8a_1$ orbital. For CH_2Cl_2 , the 1.23 eV feature is ascribed to electron capture into the empty $10a_1$ orbital. The 3.38 eV feature is ascribed to electron capture into the empty $8b_2$ orbital. For CHCl_3 , the 0.35 eV feature is ascribed to electron capture into the empty $10a_1$ orbital. The 1.83 eV feature is ascribed to electron capture into the empty $10e$ orbital. For CCl_4 , the 0.94 eV feature is ascribed to electron capture into the empty $8t_2$ orbital. To sum up, our stabilization calculations can provide support for the assignments of the features observed in the ETS of the chloromethanes.^{4,8,9}

Finally, Mulliken population analyses³⁴ have been performed for the $\omega\text{B97XD}/6\text{-}311++\text{G}(\text{d,p})$ wave functions to explain why vertical electron capture occurs at lower energy for CCl_4 . The analyses give charges of +0.54e, −0.73e, −0.77e, and −0.62e on the carbon atoms and −0.14e, 0.15e, 0.15e, and 0.05e on the chlorine atoms for CCl_4 , CHCl_3 , CH_2Cl_2 , and CH_3Cl , respectively. As can be seen from above, the carbon atom of the CCl_4 is positively charged, whereas the carbon atoms in the other molecules are negatively charged. As a result, the positively charged carbon may stabilize the resonances of CCl_4 . Interestingly enough, previous SKT studies by Jordan et al. have also indicated that *n*-perfluoroalkanes, which have a positively charged carbon backbone, also possess relatively low-lying resonance states.^{11c} Hence, it is worth studying in the future if this property is shared by haloalkanes.

4. CONCLUSIONS

The energies and lifetimes of temporary anion states of chloromethanes have been studied in this article. The obtained results have demonstrated that using SKT to calculate DOS via LRC-DFT can yield resonance parameters that are not only in agreement with experimental data and previous calculations but also more complete. For the lowest unfilled orbitals, results have indicated that the energies will decrease and lifetimes will increase with the increasing number of chlorine atoms. The

Table 3. Resonance Energies (E_r) and Widths (Γ) (eV) for Chloromethanes Using SKT ^{ω B97XD} Method with Basis Set A1

		CH ₃ Cl			CH ₂ Cl ₂				CHCl ₃			CCl ₄	
method		8a ₁	4e	9a ₁	10a ₁	8b ₂	4b ₁	11a ₁	10a ₁	10e	11a ₁	7a ₁	8t ₂
SKT ^{ωB97XD^a}	<i>E_r</i>	3.76	5.52	9.02	1.20	2.98	5.98	8.72	0.39	2.08	4.02	−0.20	1.24
	Γ	2.64	0.42	0.68	0.96	0.67	0.04	1.41	0.01	0.76	0.45		0.35
SKT ^{ωB97XD^b}	<i>E_r</i>	3.76	5.52	8.47	1.42	3.14	6.09	7.93	0.59	2.09	4.34	−0.20	1.36
	Γ	2.64	0.42	1.22	0.78	0.79	0.25	1.18	0.26	0.76	0.89		0.41
theory ^c	<i>E_r</i>	3.55			1.15	3.35			0.35	1.95		−1.10	1.05
theory ^d	<i>E_r</i>	3.25			1.51	2.68			0.36	1.84		−0.50	0.94
exptl ^e	<i>E_r</i>	3.45			1.23	3.38			0.35	1.83		<0	0.94
	Γ	2.3											
exptl ^f	<i>E_r</i>	3.45			1.01	3.17			0.42	1.83		<0	0.94
	Γ	3.05			0.92	1.29			0.40	1.4			
exptl ^g	<i>E_r</i>	3.5	5.5	8.5									
	Γ	2.6											

^aResults derived from the best Lorentzian fitting curve. ^bResults derived from the average of all Lorentzian fitting curves. ^cRef 8. ^dRef 9. ^eRef 4. ^fRef 5e. ^gRef 5d.

reasons for the effectiveness of our proposed method are due to (1) distinguishability of the temporary anion solutions from the ODC ones by the SKT, (2) the adoption of LRC-DFT so as to reduce the asymptotic behavior error, and (3) the invoking of DOS procedure. Hence, it is believed that our novel approach should be very useful in determining the energies and lifetimes of temporary anion states for chlorinated hydrocarbons.

AUTHOR INFORMATION

Corresponding Author

*Tel: 011-886-4-23590248-102. Fax: 011-886-4-23590426. E-mail: hycheng@thu.edu.tw.

Notes

The authors declare no competing financial interest.

ACKNOWLEDGMENTS

We would like to thank the reviewers for valuable comments during the revision process. This work was supported by National Science Council of the Republic of China under grant number NSC 101-2113-M-029-004.

REFERENCES

- (1) (a) Burrow, P. D.; Gallup, G. A.; Fabrikant, I. I.; Jordan, K. D. *Aust. J. Phys.* **1996**, *49*, 403. (b) Krawczyk, K.; Ulejczyk, B. *Plasma Chem. Plasma Process.* **2003**, *23*, 265.
- (2) (a) Simons, J. *J. Phys. Chem. A* **2008**, *112*, 6401. (b) Simons, J. *Annu. Rev. Phys. Chem.* **2011**, *62*, 107.
- (3) (a) Sanche, L.; Schulz, G. J. *Phys. Rev. A* **1972**, *5*, 1672. (b) Jordan, K. D.; Burrow, P. D. *Chem. Rev.* **1987**, *87*, 557.
- (4) Burrow, P. D.; Modelli, A.; Chiu, N. S.; Jordan, K. D. *J. Chem. Phys.* **1982**, *77*, 2699.
- (5) (a) Chu, S. C.; Burrow, P. D. *Chem. Phys. Lett.* **1990**, *172*, 17. (b) Shi, X.; Stephen, T. M.; Burrow, P. D. *J. Chem. Phys.* **1992**, *96*, 4037. (c) Pearl, D. M.; Burrow, P. D. *J. Chem. Phys.* **1994**, *101*, 2940. (d) Shi, X.; Chan, V. K.; Gallup, G. A.; Burrow, P. D. *J. Chem. Phys.* **1996**, *104*, 1855. (e) Aflatooni, K.; Burrow, P. D. *Int. J. Mass Spectrom.* **2011**, *205*, 149. (f) Gallup, G. A.; Fabrikant, I. I. *J. Chem. Phys.* **2011**, *135*, 134316.
- (6) (a) Benitez, A.; Moore, J. H.; Tossell, J. A. *J. Chem. Phys.* **1988**, *88*, 6691. (b) Wan, H.-X.; Moore, J. H.; Tossell, J. A. *J. Chem. Phys.* **1991**, *94*, 1868.
- (7) (a) Spence, D.; Schulz, G. J. *J. Chem. Phys.* **1973**, *58*, 1800. (b) Benassi, R.; Bernardi, F.; Bottoni, A.; Robb, M. A.; Taddei, F. *Chem. Phys. Lett.* **1989**, *161*, 79.
- (8) Falcetta, M. F.; Jordan, K. D. *J. Phys. Chem.* **1990**, *94*, 5666.

(9) Guerra, M.; Jones, D.; Distefano, G.; Scagnolari, F.; Modelli, A. *J. Chem. Phys.* **1991**, *94*, 484.

(10) Koopmans, T. *Physica* **1934**, *1*, 104.

(11) (a) Falcetta, M. F.; Jordan, K. D. *J. Am. Chem. Soc.* **1991**, *113*, 2903. (b) Falcetta, M. F.; Jordan, K. D. *Chem. Phys. Lett.* **1999**, *300*, 588. (c) Falcetta, M. F.; Choi, Y.; Jordan, K. D. *J. Phys. Chem. A* **2000**, *104*, 9605.

(12) Burrow, P. D.; Howard, A. E.; Johnston, A. R.; Jordan, K. D. *J. Phys. Chem.* **1992**, *96*, 7570.

(13) (a) Juang, C.-Y.; Chao, J. S.-Y. *J. Phys. Chem.* **1994**, *98*, 13506.

(b) Chen, C.-S.; Feng, T.-H.; Chao, J. S.-Y. *J. Phys. Chem.* **1995**, *99*, 8629. (c) Wei, Y.-H.; Cheng, H.-Y. *J. Phys. Chem. A* **1998**, *102*, 3560.

(14) (a) Hazi, A. U.; Taylor, H. S. *Phys. Rev. A* **1970**, *1*, 1109. (b) Taylor, H. S. *Adv. Chem. Phys.* **1970**, *18*, 91. (c) Fels, M. F.; Hazi, A. U. *Phys. Rev. A* **1972**, *5*, 1236. (d) Taylor, H. S.; Hazi, A. U. *Phys. Rev. A* **1976**, *14*, 2071.

(15) (a) Falcetta, M. F.; Jordan, K. D. *J. Phys. Chem.* **1990**, *94*, 5666.

(b) Falcetta, M. F.; Jordan, K. D. *J. Am. Chem. Soc.* **1991**, *113*, 2903.

(c) Falcetta, M. F.; Jordan, K. D. *Chem. Phys. Lett.* **1999**, *300*, 588.

(d) Falcetta, M. F.; Choi, Y.; Jordan, K. D. *J. Phys. Chem. A* **2000**, *104*, 9605.

(16) (a) Juang, C.-Y.; Chao, J. S.-Y. *J. Phys. Chem.* **1994**, *98*, 13506.

(b) Chen, C.-S.; Feng, T.-H.; Chao, J. S.-Y. *J. Phys. Chem.* **1995**, *99*, 8629. (c) Wei, Y.-H.; Cheng, H.-Y. *J. Phys. Chem. A* **1998**, *102*, 3560.

(17) Kohn, W.; Sham, L. *J. Phys. Rev. A* **1965**, *140*, 1133.

(18) Rienstra-Kiracofe, J. C.; Tschumper, G. S.; Schaefer, H. F., III; Nandii, S.; Ellison, G. B. *Chem. Rev.* **2002**, *102*, 231.

(19) (a) Tozer, D. J.; De Proft, F. *J. Phys. Chem. A* **2005**, *109*, 8923.

(b) De Proft, F.; Sablon, N.; Tozer, D. J.; Geerlings, P. *Faraday Discuss.* **2007**, *135*, 151. (c) Sablon, N.; De Proft, F.; Geerlings, P.; Tozer, D. J. *Phys. Chem. Chem. Phys.* **2007**, *9*, 5880. (d) Tozer, D. J.; De Proft, F. *J. Chem. Phys.* **2007**, *127*, 034108. (e) Peach, M. J. G.; De Proft, F.; Tozer, D. J. *J. Phys. Chem. Lett.* **2010**, *1*, 2826. (f) Hajgató, B.; Deleuze, M. S.; Tozer, D. J.; De Proft, F. *J. Chem. Phys.* **2008**, *129*, 084308. (h) Borgoo, A.; Tozer, D. J. *J. Phys. Chem. A* **2012**, *116*, 5497.

(20) Chai, J.-D.; Head-Gordon, M. *Phys. Chem. Chem. Phys.* **2008**, *10*, 6615.

(21) Vydrov, O. A.; Scuseria, G. E. *J. Chem. Phys.* **2006**, *125*, 234109.

(22) Yanai, T.; Tew, D. P.; Handy, N. C. *Chem. Phys. Lett.* **2004**, *393*, 51.

(23) (a) Iikura, H.; Tsuneda, T.; Yanai, T.; Hirao, K. *J. Chem. Phys.* **2001**, *115*, 3540. (b) Tsuneda, T.; Song, J.-W.; Suzuki, S.; Hirao, K. *J. Chem. Phys.* **2010**, *113*, 174101.

(24) (a) Cheng, H.-Y.; Shih, C.-C. *J. Phys. Chem. A* **2009**, *113*, 1548. (b) Cheng, H.-Y.; Shih, C.-C.; Chang, J.-T. *J. Phys. Chem. A* **2009**, *113*, 9551. (c) Cheng, H.-Y.; Chang, J.-T.; Shih, C.-C. *J. Phys. Chem. A* **2010**, *113*, 2920. (d) Cheng, H.-Y.; Chen, C.-W.; Chang, J.-T.; Shih, C.-C. *J. Phys. Chem. A* **2011**, *115*, 84. (e) Cheng, H.-Y.; Chen, C.-W. *J.*

Phys. Chem. A **2011**, *115*, 10113. (f) Cheng, H.-Y.; Chen, C.-W.; Huang, C.-H. *J. Phys. Chem. A* **2012**, *116*, 3224.

(25) (a) Dunning, T. H., Jr. *J. Chem. Phys.* **1989**, *90*, 1007. (b) Kendall, R. A.; Dunning, T. H., Jr.; Harrison, R. J. *J. Chem. Phys.* **1992**, *96*, 6769.

(26) Results obtained by the midpoint method are comparable with the more rigorous analytic continuation method (ref 19 in ref 16a).

(27) (a) Mandelshtam, V. A.; Ravuri, T. R.; Taylor, H. S. *Phys. Rev. Lett.* **1993**, *70*, 1932. (b) Mandelshtam, V. A.; Taylor, H. S.; Ryaboy, V.; Moiseyev, N. *Phys. Rev. A* **1994**, *50*, 2764.

(28) (a) Tan, S. S.; Ho, Y. K. *Chin. J. Phys.* **1997**, *35*, 701. (b) Fang, T. K.; Ho, Y. K. *J. Phys. B* **1999**, *32*, 3863. (c) Kar, S.; Ho, Y. K. *J. Phys. B* **2004**, *37*, 3177. (d) Kar, S.; Ho, Y. K. *Chem. Phys. Lett.* **2005**, *402*, 544. (e) Kar, S.; Ho, Y. K. *J. Phys. B* **2007**, *40*, 1403. (f) Kar, S.; Ho, Y. K. *New J. Phys.* **2005**, *7*, 141. (g) Kar, S.; Ho, Y. K. *Int. J. Quantum Chem.* **2008**, *108*, 1491.

(29) (a) Grimme, S. *J. Chem. Phys.* **2006**, *124*, 034108. (b) Schwabe, T.; Grimme, S. *Phys. Chem. Chem. Phys.* **2006**, *8*, 4398. (c) Schwabe, T.; Grimme, S. *Phys. Chem. Chem. Phys.* **2007**, *9*, 3397.

(30) Frisch, M. J.; Trucks, G. W.; Schlegel, H. B.; Scuseria, G. E.; Robb, M. A.; Cheeseman, J. R.; Scalmani, G.; Barone, V.; Mennucci, B.; Petersson, G. A.; Nakatsuji, H.; Caricato, M.; Li, X.; Hratchian, H. P.; Izmaylov, A. F.; Bloino, J.; Zheng, G.; Sonnenberg, J. L.; Hada, M.; Ehara, M.; Toyota, K.; Fukuda, R.; Hasegawa, J.; Ishida, M.; Nakajima, T.; Honda, Y.; Kitao, O.; Nakai, H.; Vreven, T.; Montgomery, J. A., Jr.; Peralta, J. E.; Ogliaro, F.; Bearpark, M.; Heyd, J. J.; Brothers, E.; Kudin, K. N.; Staroverov, V. N.; Kobayashi, R.; Normand, J.; Raghavachari, K.; Rendell, A.; Burant, J. C.; Iyengar, S. S.; Tomasi, J.; Cossi, M.; Rega, N.; Millam, J. M.; Klene, M.; Knox, J. E.; Cross, J. B.; Bakken, V.; Adamo, C.; Jaramillo, J.; Gomperts, R.; Stratmann, R. E.; Yazyev, O.; Austin, A. J.; Cammi, R.; Pomelli, C.; Ochterski, J. W.; Martin, R. L.; Morokuma, K.; Zakrzewski, V. G.; Voth, G. A.; Salvador, P.; Dannenberg, J. J.; Dapprich, S.; Daniels, A. D.; Farkas, O.; Foresman, J. B.; Ortiz, J. V.; Cioslowski, J.; Fox, D. J. *Gaussian 09*, revision A.02; Gaussian, Inc.: Wallingford, CT, 2009.

(31) (a) Vydrov, O. A.; Scuseria, G. E. *J. Chem. Phys.* **2005**, *122*, 184107. (b) Dutoi, A. D.; Head-Cordan, M. *Chem. Phys. Lett.* **2006**, *422*, 230.

(32) Mach, P.; Urban, J.; Staemmler, V. *Chem. Phys.* **2009**, *356*, 164.

(33) Benassi, R.; Bernardi, F.; Bottoni, A.; Robb, M. A.; Taddei, F. *Chem. Phys. Lett.* **1989**, *161*, 79.

(34) Mulliken, R. S. *J. Chem. Phys.* **1955**, *23*, 1833.